Functional analysis of miR-21-3p, miR-30b-5p and miR-150-5p shuttled by extracellular vesicles from diabetic subjects reveals their association with diabetic retinopathy

Accepted Manuscript

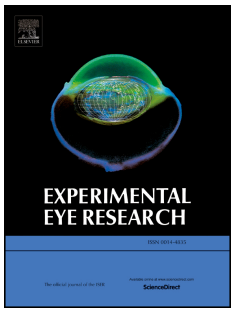

Functional analysis of miR-21-3p, miR-30b-5p and miR-150-5p shuttled by extracellular vesicles from diabetic subjects reveals their association with diabetic retinopathy

Aurora Mazzeo, Tatiana Lopatina, Chiara Gai, Marina Trento, Massimo Porta, Elena Beltramo

PII: S0014-4835(18)30837-6

DOI: https://doi.org/10.1016/j.exer.2019.04.015

Reference: YEXER 7647

To appear in: *Experimental Eye Research*

Received Date: 16 November 2018

Revised Date: 12 April 2019

Accepted Date: 15 April 2019

Please cite this article as: Mazzeo, A., Lopatina, T., Gai, C., Trento, M., Porta, M., Beltramo, E., Functional analysis of miR-21-3p, miR-30b-5p and miR-150-5p shuttled by extracellular vesicles from diabetic subjects reveals their association with diabetic retinopathy, *Experimental Eye Research* (2019), doi: https://doi.org/10.1016/j.exer.2019.04.015.

Functional analysis of miR-21-3p, miR-30b-5p and miR-150-5p shuttled by extracellular vesicles from diabetic subjects reveals their association with diabetic retinopathy

Aurora Mazzeo, Tatiana Lopatina, Chiara Gai, Marina Trento, Massimo Porta, Elena Beltramo*
Dept of Medical Sciences, University of Turin, Italy

***Email addresses**: aurora.mazzeo@unito.it* (A. Mazzeo), *t.lopatina@gmail.com* (T. Lopatina), *chiara.gai@unito.it* (C. Gai), *marina.trento@unito.it* (M. Trento), *massimo.porta@unito.it* (M. Porta), *elena.beltramo@unito.it* (E. Beltramo)

Corresponding author:

Elena Beltramo, MSc PhD, Dept of Medical Sciences, University of Turin, Corso Dogliotti 14, 10126 Torino – Italy. Tel +39.011.6708471, Fax +39.011.2368471, *elena.beltramo@unito.it*

Abstract

Microvascular dysfunctions due to altered interactions between endothelial cells (ECs) and pericytes are key-events in the pathogenesis of diabetic retinopathy. Extracellular vesicles (EVs) derived from mesenchymal stem cells cultured in diabetic-like conditions enter pericytes, cause their detachment and migration, and stimulate angiogenesis. We recently showed that EVs from diabetic patients with retinopathy have different miRNA profiling patterns from healthy controls, and determine features of retinopathy in *in vitro* models of retinal microvasculature. In particular, a role for intra-vesicle miR-150-5p, miR-21-3p and miR-30b-5p was hypothesized. In this work, we further characterized EVs from subjects with diabetic retinopathy and investigated miR-150-5p, miR-21-3p and miR-30b-5p functions inside microvascular cells. Human retinal pericytes and ECs were transfected with mimics or inhibitors, as appropriate, of miR-21-3p, miR-30b-5p and miR-150-5p, to evaluate their ability in promoting cell migration and tube formation. mRNA and protein profiling of EVs extracted from diabetic subjects with (DR group) or without retinopathy (noDR group), and healthy controls (CTR group) were also performed. Modulation of miR-150-5p, miR-21-3p and miR-30b-5p inside microvascular cells confirmed their involvement in abnormal angiogenesis. mRNA analysis revealed differing expression of 7 genes involved in angiogenesis, while subsequent protein analysis confirmed increased expression of HIF-1α in DR group. Since all these molecules are involved in the hypoxia-induced retinal damage characteristic of the disease, our data reinforce the hypothesis of a potential use of miR-150-5p, miR-21-3p and miR-30b-5p extracted from circulating EVs as prognostic biomarkers for diabetic retinopathy.

Keywords: diabetic retinopathy; extracellular vesicles; angiogenesis; hypoxia; miR-150-5p; miR-21-3p; miR-30b-5p; HIF-1α

Abbreviations: Ang1, angiopoietin-1; Ago2, argonaute 2; ApoA1, apolipoprotein A1; CCL11, eotaxin; CTR, group of healthy controls; DR, group of diabetic patients with retinopathy; EC, endothelial cell; ECM, extracellular matrix; ENG, endoglin; EV, extracellular vesicles; GM130, Golgin subfamily A member 2; HMEC, human microvascular endothelial cells; HRP, human retinal pericytes; HIF-1α, hypoxia-inducible factor 1 α; miRNA, miR, microRNA; MISEV, Minimal information for studies of extracellular vesicles; MSC, mesenchymal stem cells; noDR, group of diabetic patients without retinopathy; NRP1, neuropilin-1; TIE1, tyrosine kinase with Ig and EGF (epidermal growth factor) homology domains (angiopoietin receptor); TIMP1, tissue inhibitor of metalloproteinases; TSG101, Tumor Susceptibility Gene 101;VEGF, vascular endothelial growth factor; VEGFR1/2, vascular endothelial growth factor receptor 1/2

1. Introduction

Microvascular dysfunction due to altered interactions between endothelial cells (ECs) and pericytes are early events in the pathogenesis of diabetic retinopathy, eventually leading to abnormal angiogenesis. Extracellular vesicles (EVs) are small membrane particles, containing microRNAs (miRNAs), mRNAs, proteins and lipids, and carrying information from cell to cell (Camussi et al., 2010). They are released into the blood flow by several cell types, especially in stress conditions, including diabetes (Müller, 2012). Increased EV concentrations in the plasma of diabetic patients have been reported (Feng et al., 2009; Müller, 2012; Mazzeo et al., 2018). EVs could play a role in vascular complications, such as diabetic retinopathy, since they can influence vascular permeability and angiogenesis (Müller, 2012). Therefore, they could be investigated as potential biomarkers of the disease.

MiRNAs are small non-coding nucleotide sequences, which exercise a negative regulatory effect on their target mRNAs (Fabbri et al., 2008). They can be shuttled by EVs from cell to cell (Valadi et al., 2007) and are often related to a pathological state. In fact, they are currently under investigation as biomarkers of chronic diseases, such as diabetes (Guay and Regazzi, 2013; Snowhite et al., 2017), and diabetic retinopathy (Mastropasqua et al., 2014).

We demonstrated that EVs derived from mesenchymal stem cells cultured in diabetic-like conditions enter the pericytes, cause their detachment and migration, and stimulate angiogenesis (Beltramo et al, 2014; Mazzeo et al., 2015). We have also shown that circulating EVs from diabetic patients with retinopathy have different miRNA profiling patterns from those of both diabetic subjects without complications and healthy controls. In particular, EVs derived from patients with diabetic retinopathy are able to determine pathological changes in microvascular cells compatible with those characteristics of the disease. We hypothesized that intra-vesicle miR-150-5p, miR-21-3p and miR-30b-5p could be novel potential biomarkers for the onset and progression of diabetic retinopathy (Mazzeo et al., 2018).

In this work, we aimed at further characterizing EVs extracted by diabetic subjects with or without retinopathy and healthy controls, by addressing their mRNA and protein content. In addition, we investigated the functions and mechanisms of miR-150-5p, miR-21-3p and miR-30b-5p inside microvascular cells, by selectively inhibiting or mimicking their action to better evaluate their role in vessel homeostasis.

2. Materials and methods

2.1 Subjects

Three age- and gender-matched groups were examined: 7 type 1 subjects (DR group) with proliferative diabetic retinopathy, but no other complications of diabetes, systemic or autoimmune diseases; 7 diabetic subjects without retinopathy (noDR group) and 7 healthy controls (CTR group). The subject characteristics are described in Mazzeo et al. (2018). Informed consent was obtained from all participants, and ethical clearance for involvement of human subjects in research was obtained from the *Comitato Etico Interaziendale A.O.U. Città della Salute e della Scienza di Torino - A.O. Ordine Mauriziano - A.S.L. TO1*. Overnight fasting venous blood samples were collected in tubes containing EDTA for plasma separation.

2.2 Cell cultures

A stabilized human retinal pericyte line (HRPs) is currently available in our laboratory (Berrone et al., 2009), while human microvascular ECs (HMECs) were purchased from Lonza (Basel, Switzerland). HRPs were

cultured in DMEM + 10% FCS, while HMECs in EBM-2 growth medium (Lonza). When used in the experiments, both HRPs and HMECs were maintained in DMEM + 10% FCS. Reagents for cell cultures were purchased from Sigma-Aldrich (St Louis, MO, USA).

2.3 EV separation and characterization

EVs were separated from plasma samples by two-step centrifugation: at 3000 *g* for 30 min to remove debris, apoptotic bodies and platelets, and at 100,000 *g* (average *g* at the middle of the tube, speed 40164 rpm, K-factor 125) for 3 hrs at 4°C of the cell-free supernatants (*ultracentrifuge Optima L-100K,* equipped with *rotor 90 Ti, 90000 rpm, fixed angle*, Beckman Coulter, Brea, CA, USA). EVs were either used immediately or stored at −80°C in DMEM + 5% dimethyl-sulfoxide. Fresh and stored EVs showed no differences in biological activity. EV size, distribution and number were evaluated through a NanoSight LM10 (NanoSight Ltd, Minton Park, UK), running the Nanoparticle Tracking Analysis 2.3 software, while surface markers by FACS (Guava easyCyte™ Flow Cytometer, Millipore, Burlington, MA, USA), as described in Mazzeo et al. (2018). In addition, EVs were analyzed by Western blotting for the presence/absence of the EV markers/contaminants CD63 (sc-5275, Santa Cruz Biotechnology Dallas, TX, USA), Tumor Susceptibility Gene 101 (TSG101, sc-101254, Santa Cruz Biotechnology), apolipoprotein A1 (ApoA1, ab52945, Abcam, Cambridge, UK) and Golgin subfamily A member 2 (GM130, ab52945, Abcam) (**Suppl. Mat.1, Fig. 1**).

To control the efficacy of our isolation method, EV samples from the 3 groups were also separated by OptiPrep™ (Sigma-Aldrich), through a modification of the method described by Collino et al. (2017). Briefly, gradient was formed by layering 2.5 ml of 40%, 2.5 ml of 20%, 2.5 ml of 10%, and 2 ml of 5% iodixanol gradient solution in polycarbonate tubes. 500 µl EVs were overlaid onto the top of the gradient, and tubes were centrifuged for 18h at 100,000 g at 4°C. Ten gradient fractions of 1 mL were collected from the top of the tube and the density of each fraction was measured by weighing a fixed volume. Each fraction was diluted with 10 ml PBS and further centrifuged at 100,000 g for 2h at 4°C. Pellets were re-suspended in 100 µl PBS and used freshly. Combined fractions 4-6 were chosen for experiments, the density of them being 1.11-1.13 g/ml, similar to the density range of small EVs separated by iodixanol gradient (1.115–1.145 g/mL) (Kowal et al., 2016).

The expression of the contaminants ApoA1 and Argonaute 2 (Ago2, ab57113, Abcam) was analysed in both ultracentrifugation and OptiPrep™ EVs and compared with whole plasma (**Suppl. Mat.1, Fig. 2**). MiR21-3p, miR30b-5p and miR150-5p expressions were assessed by qRT-PCR in OptiPrep™ EV samples from the 3 groups (**Suppl. Mat. 1, Fig. 3**).

2.4 Cell transfection

To induce miR-21-3p and miR-30b-5p overexpression, subconfluent HRP/HMEC cultures were transiently transfected using *HiPerFect Transfection Reagent* (Qiagen, Hilden, Germany), with 5 nM miRNA mimics (*Syn-hsa-miR-21-3p*, MSY0004494, and *Syn-hsa-miR-30b-5p*, MSY0000420, Qiagen). Negative control cultures were transfected with *Allstars Negative Control SiRNA* (Qiagen). MiR-150-5p inhibition was obtained by adding to cell cultures 50 nM *anti-hsa-Mir-150-5p* (MIN0000451, Qiagen), or *miScript Inhibitor Negative Control* (Qiagen) for negative controls, according to manufacturer's instructions. Cells were also transfected with the mimics and antagomir all together. Transfection efficiency was assessed by RT-qPCR after 24-48 hrs (**Suppl. Mat. 1, Fig.4**).

2.5 Cell migration

Transfected HRPs or HMECs were seeded inside 8 µm pore polycarbonate membranes. After 24 hrs their migration rate was measured using the colorimetric *QCM Chemotaxis Cell Migration Assay* (Merck-

Millipore, Darmstadt, Germany). Cells still inside the insert were removed and those migrated through the membrane stained. The stain was subsequently extracted and transferred to a 96-well ELISA plate for colorimetric reading at 560 nm.

2.6 Vessel-like formation assay

15,000 transfected HRPs and 15,000 transfected HMECs were seeded together onto Matrigel-coated 24-well plates and cultured in DMEM. Co-cultures of non-transfected cells, as a control, were also established. After 24 and 48 hr incubation, phase-contrast photos at 100x magnification of five random fields per each well were captured. The total length of the network structures in each field was measured using the MicroImage analysis system (Casti Imaging, Venice, Italy), as previously described (Bussolati et al., 2003). Mean of the 5 fields of each well was calculated. Each measure was performed in duplicate wells and expressed as ratio of control (non-transfected cells).

2.7 mRNA profiling

mRNA profiling was performed on plasma EVs from 4 subjects in each group, chosen as the best matches with their correspondent subjects in the other two groups, to reduce as much as possible individual variations. Total RNA was extracted from EVs using *mirVana RNA Isolation kit* (Thermo Fisher Scientific, Waltham, MA, USA) and quantified spectrophotometrically (Nanodrop ND-1000, Wilmington, DE, USA). 50 ng of total RNA were retro-transcribed to cDNA and pre-amplified using *RT^2 PreAMP cDNA Synthesis Kit* (Qiagen). Expression of 84 genes involved in angiogenesis was evaluated using the *RT² Profiler™ PCR Array Human Angiogenesis* (PAHS-024Z) (Qiagen), according to the manufacturer's instructions. qRT-PCR was performed using *QuantStudioTM 12K Flex Real-Time PCR System* (Applied Biosystems). Relative gene expression was determined using the $2^{-\Delta\Delta CT}$ method.

To validate the 7 mRNAs found to be differentially expressed, qRT-PCR was performed on plasma EVs from all individuals (7 subjects per each group). Total RNA was extracted using the *mirVana RNA Isolation Kit* and quantified spectrophotometrically. 50 ng of RNA were reverse-transcribed using *High Capacity cDNA Reverse Transcription Kits* (Thermo Fisher Scientific) and qRT-PCR performed using *Power SYBR™ Green PCR Master Mix*, by the *QuantStudioTM 12K Flex Real-Time PCR System*. mRNA expression was normalized against beta-2-microglobulin.

2.8 Protein extraction

To extract total proteins, EVs were lysed using *M-PER Mammalian Protein extraction reagent* (ThermoFisher) added with 10 µl/ml protease inhibitor cocktail kit (ThermoFisher). Extracts were kept ice-cold and cleared by centrifugation at 20,000 g for 15 min at 4°C. Protein concentration was determined using the Bradford method. Supernatants were stored at −80°C.

2.9 Western blot analysis

30 µg proteins were loaded on pre-cast gels (4–15% Mini-PROTEAN® TGX™ Precast Gel, Bio-Rad, Irvine, CA, USA), separated by electrophoresis and transferred to nitrocellulose membranes. Immunoblotting was performed by incubating the membranes with specific antibodies, according to the manufacturer's instructions.

All primary antibodies were used at a 1:1000 dilution. Immunoreactive bands were visualized using the enhanced chemiluminescence (ECL) Western blotting protocol (Merck-Millipore). Antibodies used were: anti-HIF-1α (sc-8711, Santa Cruz Biotechnology), anti-Ang1 (sc-74528, Santa Cruz Biotechnology) and anti-β-actin (sc-47778, Santa Cruz Biotechnology).

The relative signal strength was quantified by densitometric analysis (ImageJ software, NIH, USA), and values normalized against β-actin.

2.10 Statistical analysis

Statistical comparisons among groups were carried out by one-way ANOVA with Bonferroni *post-hoc* correction. Results were considered significant for p≤0.05. SPSS software version 24.0 (IBM) was used for statistical analysis.

3. Results

3.1 EV characterization

EV size, distribution and number were evaluated through NanoSight, and their surface markers by flow cytometry, as already described in Mazzeo et al. (2018). In addition, we further analysed EVs by WB for the presence/absence of EV markers/contaminants, choosing one protein from each category suggested by the Minimal information for studies of extracellular vesicles (MISEV) Guidelines 2018 (Théry et al., 2018): a transmembrane protein (CD63), a cytosolic protein (TSG101), the contaminant ApoA1 abundant in plasma, and GM130, whose absence demonstrates the specificity of EVs to the small EV subtypes (<200nm). Our results show the presence of the positive EV markers CD63 and TSG101, the depletion of ApoA1 in comparison with whole plasma, and the absence of GM130 (**Suppl. Mat. 1, Fig. 1**). To further check the efficacy of our isolation method, EV samples from the 3 groups were separated by both ultracentrifugation and OptiPrep™ and the expression of the contaminants ApoA1 and Ago2 compared with whole plasma. The mean OptiPrep™ – separated EV size was respectively 162±24 nm, 167± 83, 159±33 nm in the 3 groups (CTR, noDR, DR), comparable with those extracted by ultracentrifugation and described in Mazzeo et al. (2018). We found ApoA1 and Ago2 expressed in ultracentrifugation- and OptiPrep™ – separated EVs from all groups, but their concentration was much lower than in plasma, in accordance with MISEV Guidelines 2018 recommendations (**Suppl. Mat.1, Fig. 2a**). Moreover, normalizing densitometric values to CD63, a positive EV marker, we found no differences in Ago2 and ApoA1 concentrations between UC- and OptiPrep™-separated EVs (**Suppl. Mat. 1, Fig. 2b-c**). Finally, miR21-3p, miR30b-5p and miR150-5p expression in OptiPrep™-isolated EVs showed the same increase/decrease we had previously found in EVs separated by ultracentrifugation (Mazzeo et al, 2018) (**Suppl. Mat. 1, Fig. 3**).

3.2 Transfection with miRNA mimics/antagomir increases HRP migration and HMEC/HRP vessel-like formation

In our previous study (Mazzeo et al., 2018), we had found increased miR-21-3p and miR-30b-5p, and decreased miR-150-5-p inside EVs from diabetic patients with diabetic retinopathy; therefore, we transfected HMECs and HRPs with specific mimics/inhibitor (antagomir), as appropriate, for these miRNAs, to evaluate their functional role. In addition, we transfected cells with all mimics/antagomir together, to better evaluate the possible synergistic/antagonistic effects of the 3 miRNAs in the human subjects. Transfection efficiency was assessed after 24-48 hrs (**Suppl. Mat.1, Fig. 4**).

No effects on HMEC migration following transfection were noticed (**Fig. 1a**), while HRP migration was increased in all cases: +53% vs non-transfected cells following miR-150-5p inhibition (p=0.005), +83% after miR21-3p-mimic transfection (p<0.05), +65% after miR30-b-5p-mimic transfection (p<0.05), and +80% (p<0.05) after transfection with all mimics/antagomir together (**Fig. 1b**).

Similarly, vessel-like formation in HMEC/HRP co-cultures in Matrigel was increased following transfection in all cases: +59% with miR-150-5p inhibitor vs non-transfected cells (p<0.05 vs non-transfected cells), +74% with miR-21-3p-mimic (p<0.05), +233% with miR30-b-5p-mimic (p<0.05), and +698% after transfection with all mimics/antagomir together (p<0.05 vs non-transfected cells and all single transfections) (**Fig. 2**).

3.3 mRNA and protein profiling

We examined the mRNA expression of 84 key-genes involved in the modulation of angiogenesis in plasma EVs derived from our 3 groups of subjects. Array analysis revealed 7 mRNAs to be differentially expressed in the 3 groups, especially as regards the DR group in comparison with healthy controls (CTR). In particular, 5 of them were downregulated in DR vs CTR (p<0.05): angiopoietin-1 (Ang1), endoglin (ENG), neuropilin-1 (NRP1), the angiopoietin receptor TIE1, and the tissue inhibitor of metalloproteinases (TIMP1). Eotaxin (CCL11) was downregulated in the noDR subjects vs CTR (p<0.05), while hypoxia-inducible factor 1α (HIF-1α) was more than 2-fold upregulated in DR patients vs healthy controls (p<0.05) (**Fig. 3**). A complete list of the mRNAs expressed in the 3 groups without significant differences is shown in **Suppl. Mat. 2**.

Subsequently, the expression of the differentially expressed mRNAs was investigated by qRT-PCR in all subjects (7 per each group). Ang1 was confirmed decreased in the DR group in comparison with healthy controls (-86%, p<0.005) (**Fig. 4a**), while HIF-1α was 2.5 fold higher in the noDR group and 3-fold higher in the DR group in comparison with controls (p<0.05 in both cases) (**Fig. 4b**).

Ang1 and HIF-1α protein expression was also evaluated. While HIF-1α protein expression concurred with mRNA expression (+63 and +140% in no DR and DR groups in comparison with CTR, p<0.05 in DR/noDR vs CTR and in DR vs noDR) (**Fig.4 d,f**), Ang1 protein expression was unchanged among the groups (**Fig. 4c,e**).

4. Discussion

Reliable and specific biomarkers for prognosis and prevention of diabetes and its complications are certainly needed. In this paper, we further addressed the molecular composition of circulating EVs from DR patients, in order to gain further insight in their characterization and evaluated the functional role of miR-150-5p, miR-21-3p and miR-30b-5p in retinal microvascular cells. Our results support a role for intra-vesicle miR-150-5p, miR-21-3p and miR-30b-5p in diabetic retinopathy and their association with the hypoxic environment typical of this complication.

A potential pitfall of this work may be the method of separation of EVs from plasma. There is no general consensus in the literature about the best protocol to isolate EVs. We are aware that ultracentrifugation does not result in a particularly pure EV preparation, but it is currently still commonly used. Other methods are much more challenging, time-consuming and operator-dependent and, therefore, scarcely applicable to routine clinical practice (Kalra et al., 2013). Moreover, according to MISEV guidelines, a complete separation and purification of EVs from possible contaminants, such as lipoproteins or Ago2, is currently rather impossible to achieve (Théry et al., 2018). To check the efficacy of our separation method, we compared a set of EVs from the 3 groups isolated by OptiPrep™ with EVs separated by ultracentrifugation, and found comparable presence of ApoA1 and Ago2, much lower in both cases than in whole plasma. In addition, we found superimposable expressions of the three miRNAs of interest to those we previously described in ultracentrifugation-separated EVs (Mazzeo et al. 2108). Finally, in accordance with the MISEV Guidelines 2018 (Théry et al., 2018), we further analyzed EVs separated by ultracentrifugation for the

expression of the EV markers CD63 and TSG101, and the absence of GM130, the latter demonstrating their specificity to the small EV subtypes (< 200 nm).

We have previously demonstrated that circulating EVs from patients with diabetic retinopathy induce features of retinopathy in *in vitro* models of retinal microvasculature, such as pericyte detachment and migration, new vessel formation and increased retinal-blood barrier permeability. Moreover, we found molecular differences in EVs from DR subjects when compared to healthy controls and non-complicated diabetic patients, hypothesizing a role for miR-150-5p, miR-21-3p and miR-30b-5p as potential biomarkers of the onset of diabetic retinopathy (Mazzeo et al., 2018). Previous reports in the literature have already postulated a role for miR-150-5p, highlighting its ability to inhibit angiogenic factors *in vitro*, and showing its reduction during pathological neovascularization in mice with oxygen-induced proliferative retinopathy (Liu CH et al., 2015). On the other hand, miR-21-3p was found overexpressed in the retina of db/db mice (Chen Q et al., 2017), and to induce angiogenesis by mediating an increase in HIF-1α and VEGF expression (Báez-Vega et al., 2016; Snowhite et al., 2017). A role as a pro-angio-miRNA for miR-30b-5p, promoting EC migration and tube formation *in vitro*, has also been reported (Gong et al., 2017).

To better evaluate the possible role of miR-150-5p, miR-21-3p and miR-30b-5p, we transiently transfected pericytes and ECs with an inhibitor (antagomir) of miR150-5p, which was decreased in EVs from DR subjects, and with specific mimics of miR-21-3p and miR-30b-5p that, conversely, had been found increased. MiRNA mimics are double-stranded RNA fragments which imitate endogenous miRNA functions once transfected inside cells, while single-stranded antagomirs specifically bind to their target miRNA inhibiting it. The use of these artefacts to better understand the role of endogenous miRNAs inside the cells is well described (Krützfeldt et al., 2005; Rupaimoole and Slack, 2017) and their potential use as prognostic and therapeutic approaches for cancer (Rupaimoole and Slack, 2017*),* inflammation (Tili et al., 2013) and chronic diseases such as diabetes and even diabetic retinopathy (McArthur et al., 2011) has been postulated. In our settings, pericytes transiently transfected with mimics/antagomir showed increased migration, while the number of newly-formed vessel-like structures was amplified in transfected EC/pericyte co-cultures grown in Matrigel, especially when cells were transfected simultaneously with all mimics/antagomir together, demonstrating a strong synergistic effect of the three miRNAs together. These data strongly support the hypothesis of an involvement of miR-150-5p, miR-21-3p and miR-30b-5p in the pathogenesis of diabetic retinopathy. As regards mRNA profiling, array analysis showed that seven mRNAs related to angiogenesis were differentially expressed in the three groups, especially in the DR group compared to healthy controls, six of them downregulated, and one upregulated. However, subsequent control RT-PCR confirmed only two of them to be modulated in the different groups: Ang1, which was decreased in the DR group in comparison with controls, and HIF-1α, upregulated in both noDR and DR groups.

Ang1 involvement in angiogenesis is controversial. It is known to play a fundamental role in pericyte recruitment and vessel stabilization during embryonic life and in physiological conditions, and has been associated to tumor angiogenesis (Metheny-Barlow and Li, 2003; Shim et al., 2007). On the other hand, its role in vessel stabilization may limit abnormal neo-vascularization and overexpression of Ang1 has been reported to inhibit tumor growth in different types of cancer (Metheny-Barlow and Li, 2003; Shim et al., 2007). A protective role for Ang1 in diabetic retinopathy has also been postulated. In fact, Ang1 has been demonstrated to promote healthy vessel formation while inhibiting abnormal angiogenesis, impaired permeability and even neurodegeneration in oxygen-induced retinopathic mice (Lee et al., 2013), while a single-dose intra-vitreal injection of Ang1 vehiculated by an adeno-associated virus serotype 2 was able to prevent neurovascular pathology and promote vascular regeneration in a mouse model of diabetic

retinopathy (Cahoon et al., 2015). Reduced Ang1 secretion was also described in retinal endothelial cells grown in high glucose concentrations (Stewart et al., 2016). Therefore, the decreased Ang1 mRNA expression we found in EVs derived from DR patients might play a role in pericyte loss, vessel destabilization and, potentially, increased neo-angiogenesis. However, Ang1 protein expression inside EVs was unchanged among the three groups. Differences between mRNA and protein expression often occur and can be ascribed to the complex cell regulation mechanisms at transcriptional and/or translational level and to the different half-lives of mRNA and proteins inside the cytoplasm (Greenbaum et al., 2003). Thus, cells may implement strategies to counteract damages caused by pathologically low (or high) mRNA/protein levels.

Our data show also increased HIF-1 α mRNA and protein expression in EVs derived from both the noDR and DR groups, in comparison to healthy control. Moreover, HIF-1 α protein expression in EVs from the DR group was significantly higher also in comparison with the noDR group. HIF-1α role in angiogenesis and diabetic retinopathy is well known. The hypoxic environment inside the diabetic eyes leads to the activation of HIF-1α, which translocates inside the nucleus and activates target genes such as VEGF (D'Amico et al., 2018). This, in turn, is a potent pro-angiogenic factor and currently the main target of diabetic retinopathy therapy (Bandello et al., 2013). We previously described an increase in HIF-1α and VEGF, following a concomitant decrease in miR-126, in human retinal pericytes exposed to EVs extracted by mesenchymal stem cells cultured in a hyperglycemic/hypoxic milieu (Mazzeo et al., 2015). In hypoxic conditions, increased HIF-1α activates several miRNAs, among which miR-30b-5p (Camps et al., 2014; Choudhry and Mole, 2016) and miR-21 (Liu Y et al., 2014; Choudhry and Mole, 2016). In turn, miR-21-3p promotes angiogenesis through AKT and ERK activation and increased HIF-1α expression (Liu LZ et al., 2011, Báez-Vega et al., 2016; Snowhite et al., 2017), while miR-30b-5p directly induces *in vitro* EC migration and tube formation (Gong et al., 2017) . Moreover, a recent report correlates miR-150-5p with HIF-1α through *ITGA6*, a gene overexpressed in cancer and involved in cancer cell migration and invasion, and whose expression is downregulated by miR-150-5p and upregulated by HIF-1α (Koshizuka et al., 2017). Thus, decreased miR-150-5p and increased miR-21-3p, miR-30b-5p and HIF-1α, as we found in EVs derived from DR subjects, may all together concur to vessel destabilization and angiogenesis. The fact that all these molecules are involved in hypoxia-induced damage, characteristic of the diabetic eye, may explain why we found them up or downregulated in the DR group, and therefore we think that they may be taken into account as markers of diabetic retinopathy.

5. Conclusions

Our data strengthen the hypothesis of a role of miR-150-5p, miR-21-3p and miR-30b-5p in the pathogenesis of diabetic retinopathy and their strong correlation with the hypoxic environment characteristic of the disease. In addition, we would suggest that miR-150-5p, miR-21-3p and miR-30b-5p extracted from circulating EVs may have a role as prognostic biomarkers of the onset and development of this complication. Further studies are needed to confirm this hypothesis, enrolling a larger number of subjects.

Funding

This work was supported by an EFSD/Lilly Research Fellowship to AM; and by the Italian Ministry of Education, Universities and Research (MIUR, Ricerca locale ex-60% 2015 to EB).

Author Contributions

Design of the study: AM, EB, TL, MP. Selection of subjects: AM, EB, MT, MP. Experimental work, data collection and analysis: AM, EB, TL, CG. Interpretation of data: AM, EB, MP. Manuscript drafting: AM, EB. Critical revision: TL, CG, MT, MP. All authors have approved the final article.

Declarations of interest: none

References

Báez-Vega PM, Vargas IME, Valiyeva F, Encarnación-Rosado J, Roman A, Flores J, Marcos-Martínez MJ, Vivas-Mejía PE. Targeting miR-21-3p inhibits proliferation and invasion of ovarian cancer cells. Oncotarget 2016; 7:36321-37. http://doi.org/10.18632/oncotarget.9216

Bandello F, Lattanzio R, Zucchiatti I, Del Turco C. Pathophysiology and treatment of diabetic retinopathy. Acta Diabetol 2013;50:1-20. doi: 10.1007/s00592-012-0449-3

Beltramo E, Lopatina T, Berrone E, Mazzeo A, Iavello A, Camussi G, Porta M. Extracellular vesicles derived from mesenchymal stem cells induce features of diabetic retinopathy in vitro. Acta Diabetol 2014;51:1055-64. doi: 10.1007/s00592-014-0672-1

Berrone E, Beltramo E, Buttiglieri S, Tarallo S, Rosso A, Hammes HP, Porta M. Establishment and characterization of a human retinal pericyte line: a novel tool for the study of diabetic retinopathy. Int J Mol Med 2009;23:373-8. https://doi.org/10.3892/ijmm_00000141

Bussolati B, Deambrosis I, Russo S, Deregibus MC, Camussi G. Altered angiogenesis and survival in human tumor-derived endothelial cells. FASEB J 2003;17:1159-1161. doi:10.1096/fj.02-0557fje

Cahoon JM, Rai RR, Carroll LS, Uehara H, Zhang X, O'Neil CL, Medina RJ, Das SK, Muddana SK, Olson PR, Nielson S, Walker K, Flood MM, Messenger WB, Archer BJ, Barabas P, Krizaj D, Gibson CC, Li DY, Koh GY, Gao G, Stitt AW, Ambati BK. Intravitreal AAV2.COMP-Ang1 Prevents Neurovascular Degeneration in a Murine Model of Diabetic Retinopathy. Diabetes 2015;64:4247-59. doi: 10.2337/db14-1030.

Camps C, Saini HK, Mole DR, Choudhry H, Reczko M, Guerra-Assunção JA, Tian YM, Buffa FM, Harris AL, Hatzigeorgiou AG, Enright AJ, Ragoussis J. Integrated analysis of microRNA and mRNA expression and association with HIF binding reveals the complexity of microRNA expression regulation under hypoxia. Mol Cancer 2014;13:28. doi: 10.1186/1476-4598-13-28

Camussi G, Deregibus MC, Tetta C. Paracrine/endocrine mechanism of stem cells on kidney repair: role of microvesicle-mediated transfer of genetic information. Curr Opin Nephrol Hypertens 2010;19:7-12. doi: 10.1097/MNH.0b013e328332fb6f

Chen Q, Qiu F, Zhou K, Matlock HG, Takahashi Y, Rajala RVS, Yang Y, Moran E, Ma JX. Pathogenic Role of microRNA-21 in Diabetic Retinopathy Through Downregulation of PPARα. Diabetes 2017;66:1671-82. doi: 10.2337/db16-1246

Choudhry H, Mole DR. Hypoxic regulation of the noncoding genome and NEAT1. Brief Funct Genomics 2016;15:174-185. doi: 10.1093/bfgp/elv050

Collino F, Pomatto M, Bruno S, Tapparo M, Sicheng W, Quesenberry P, Camussi G. Exosome and Microvesicle-Enriched Fractions Isolated from Mesenchymal Stem Cells by Gradient Separation Showed Different Molecular Signatures and Functions on Renal Tubular Epithelial Cells. Stem Cell Rev 2017;13:226-243. doi: 10.1007/s12015-016-9713-1

D'Amico AG, Maugeri G, Rasà DM, La Cognata V, Saccone S, Federico C, Cavallaro S, D'Agata V. NAP counteracts hyperglycemia/hypoxia induced retinal pigment epithelial barrier breakdown through modulation of HIFs and VEGF expression. J Cell Physiol 2018;233:1120-1128. doi: 10.1002/jcp.25971.

Fabbri M, Croce CM, Calin GA. MicroRNAs. Cancer J 2008;14:1-6. doi: 10.1097/PPO.0b013e318164145e.

Feng B, Chen Y, Luo Y, Chen M, Li X, Ni Y. Circulating level of microparticles and their correlation with arterial elasticity and endothelium-dependent dilation in patients with type 2 diabetes mellitus. Atherosclerosis 2010;208:264-9. doi: 10.1016/j.atherosclerosis.2009.06.037

Gong M, Yu B, Wang J, Wang Y, Liu M, Paul C, Millard RW, Xiao DS, Ashraf M, Xu M. Mesenchymal stem cells release exosomes that transfer miRNAs to endothelial cells and promote angiogenesis. Oncotarget 2017;8:45200-12. doi: 10.18632/oncotarget.16778

Greenbaum D, Colangelo C, Williams K, Gerstein M. Comparing protein abundance and mRNA expression levels on a genomic scale. Genome Biology 2003;4:117 doi: 10.1186/gb-2003-4-9-117

Guay C, Regazzi R. Circulating microRNAs as novel biomarkers for diabetes mellitus. Nat Rev Endocrinol 2013; 9:513–21. doi: 10.1038/nrendo.2013.86

Kalra H, Adda CG, Liem M, Ang C, Mechler A, Simpson RJ, Hulett MD, Mathivanan S. Comparative proteomics evaluation of plasma exosome isolation techniques and assessment of the stability of exosomes in normal human blood plasma. Proteomics 2013;13:3354-3364. doi:10.1002/pmic.201300282

Koshizuka K, Nohata N, Hanazawa T, Kikkawa N, Arai T, Okato A, Fukumoto I, Katada K, Okamoto Y, Seki N. Deep sequencing-based microRNA expression signatures in head and neck squamous cell carcinoma: dual strands of pre-miR-150 as antitumor miRNAs. Oncotarget 2017;8:30288-30304. doi: 10.18632/oncotarget.16327

Kowal J, Arras G, Colombo M, Jouve M, Morath JP, Primdal-Bengtson B, Dingli F, Loew D, Tkach M, Théry C. Proteomic comparison defines novel markers to characterize heterogeneous populations of extracellular vesicle subtypes. Proc Natl Acad Sci USA 2016; 113: E968–E977. doi: 10.1073/pnas.1521230113

Krützfeldt J, Rajewsky N, Braich R, Rajeev KG, Tuschl T, Manoharan M, Stoffel M. Silencing of microRNAs in vivo with 'antagomirs'. Nature 2005; 438:685-689. doi: 10.1038/nature04303

Lee J, Kim KE, Choi DK, Jang JY, Jung JJ, Kiyonari H, Shioi G, Chang W, Suda T, Mochizuki N, Nakaoka Y, Komuro I, Yoo OJ, Koh GY. Angiopoietin-1 guides directional angiogenesis through integrin αvβ5 signaling for recovery of ischemic retinopathy. Sci Transl Med 2013;5:203ra127. doi: 10.1126/scitranslmed.3006666

Liu CH, Sun Y, Li J, Gong Y, Tian KT, Evans LP, Morss PC, Fredrick TW, Saba NJ, ChenaJ. Endothelial microRNA-150 is an intrinsic suppressor of pathologic ocular neovascularization. Proc Natl Acad Sci USA 2015;112:12163-8. doi: 10.1073/pnas.1508426112

Liu LZ , Li C, Chen Q, Jing Y, Carpenter R, Jiang Y, Kung HF, Lai L, Jiang BH. MiR-21 induced angiogenesis through AKT and ERK activation and HIF-1alpha expression. PLoS One 2011; 6:e19139. doi: 10.1371/journal.pone.0019139

Liu Y, Nie H, Zhang K, Ma D, Yang G, Zheng Z, Liu K, Yu B, Zhai C, Yang S. A feedback regulatory loop between HIF-1α and miR-21 in response to hypoxia in cardiomyocytes. FEBS Lett 2014; 588:3137-3146. doi: 10.1016/j.febslet.2014.05.067

Mastropasqua R, Toto L, Cipollone F, Santovito D, Carpineto P, Mastropasqua L. Role of microRNAs in the modulation of diabetic retinopathy. Prog Retin Eye Res 2014;43:92-107 doi: 10.1016/j.preteyeres.2014.07.003

Mazzeo A, Beltramo E, Iavello A, Carpanetto A, Porta M. Molecular mechanisms of extracellular vesicle-induced vessel destabilization in diabetic retinopathy. Acta Diabetol 2015;52:1113-9. doi: 10.1007/s00592-015-0798-9

Mazzeo A, Beltramo E, Lopatina T, Gai C, Trento M, Porta M. Molecular and functional characterization of circulating extracellular vesicles from diabetic patients with and without retinopathy and healthy subjects. Exp Eye Res 2018;176:69-77. doi: 10.1016/j.exer.2018.07.003

McArthur K, Feng B, Wu Y, Chen S, Chakrabarti S. MicroRNA-200b Regulates Vascular Endothelial Growth Factor–Mediated Alterations in Diabetic Retinopathy. Diabetes 2011; 60:1314-1323. doi: 10.2337/db10-1557

Metheny-Barlow LJ, Li LY. The enigmatic role of angiopoietin-1 in tumor angiogenesis. Cell Research 2003; 13:309-317. doi: 10.1038/sj.cr.7290176

Müller G. Microvesicles/exosomes as potential novel biomarkers of metabolic diseases. Diabetes Metab Syndr Obes 2012;5:247-82. doi: 10.2147/DMSO.S32923

Rupaimoole R and Slack FJ. MicroRNA therapeutics: towards a new era for the management of cancer and other diseases. Nature Rev Drug Discovery 2017;16:203-222. doi: 10.1038/nrd.2016.246

Shim WSN, Ho IAW, Wong PEH. Angiopoietin: A TIE(d) Balance in Tumor Angiogenesis. Mol Cancer Res 2007;5:655-665. doi: 10.1158/1541-7786.MCR-07-0072

Snowhite IV, Allende G, Sosenko J, Pastori RL, Messinger Cayetano S, Pugliese A. Association of serum microRNAs with islet autoimmunity, disease progression and metabolic impairment in relatives at risk of type 1 diabetes. Diabetologia 2017;60:1409. doi:10.1007/s00125-017-4294-3

Stewart EA, Saker S, Amoaku WM. Dexamethasone reverses the effects of high glucose on human retinal endothelial cell permeability and proliferation in vitro. Exp Eye Res 2016;151:75-81. doi: 10.1016/j.exer.2016.08.005

Théry C, Witwer KW, Aikawa E, et al. Minimal information for studies of extracellular vesicles 2018 (MISEV2018): a position statement of the International Society for Extracellular Vesicles and update of the MISEV2014 guidelines. J Extracell Vesicles 2018;7:1535750. doi:10.1080/20013078.2018.1535750

Tili E, Michaille J, Croce CM. MicroRNAs play a central role in molecular dysfunctions linking inflammation with cancer. Immunol Rev 2013; 253: 167-184. doi:10.1111/imr.12050

Valadi H, Ekstrom K, Bossios A, Sjostrand M, Lee JJ, Lotvall JO. Exosome-mediated transfer of mRNAs and microRNAs is a novel mechanism of genetic exchange between cells. Nat Cell Biol 2007;9:654-659. doi:10.1038/ncb1596

Figure captions

Fig. 1 Transfection with miRNA mimics or antagomir increases HRP, but not HMEC, migration. a) HMEC, **b**) HRP. *ctrl* = non-transfected cells, *inib neg ctrl* = cells transfected with miScript Inhibitor Negative Control, *anti-miR-150-5p* = cells transfected with miR-150-5p antagomir, *mim neg ctrl* = cells transfected with Allstars Negative Control SiRNA, *mim miR-21-3p* = cells transfected with miR-21-3p mimic*, mim miR-30-5p* = cells transfected with miR-30-5p mimic, *all mimics/antagomir* = cells transfected with all mimics/antagomir. Fold increases vs *ctrl*, n=5, * *p*<=0.05 vs *ctrl* and relevant negative control.

Fig. 2 Transfection with miRNA mimics or antagomir increases *in vitro* formation of vessel-like structures by HRP/EC co-cultures. a-d) Vessel-like structure formation by **a**) non-transfected cells (ctrl); **b**) cells transfected with miR-150-5p antagomir; **c**) cells transfected with miR-21-3p mimic; **d**) cells transfected with miR-30-5p mimic. Magnification 100x. **e**) Quantitative analysis of newly-formed vessel-like structures after 24 hr in Matrigel, *ctrl* = non-transfected cells, *inib neg ctrl* = cells transfected with miScript Inhibitor Negative Control, *anti-miR-150-5p* = cells transfected with miR-150-5p antagomir, *mim neg ctrl* = cells transfected with Allstars Negative Control SiRNA, *mim miR-21-3p* = cells transfected with miR-21-3p mimic*, mim miR-30-5p* = cells transfected with miR-30-5p mimic, *all mimics/antagomir* = cells transfected with all mimics/antagomir. Fold increases vs *ctrl*, n=5, * *p*<=0.05 vs *ctrl* and relevant negative control, # *p*<0.05 *vs* anti-miR-150-5p, mim miR-21-3p and mim miR30-5p.

Fig. 3 mRNA profiling in plasma EVs extracted from healthy subjects (**CTR**) and from diabetic patients without (**noDR**) and with retinopathy (**DR**), expression of the 7 differentially expressed mRNAs, fold increases vs the control group (CTR). *White bars*: CTR, *light grey bars*: noDR, *dark grey bars*: DR. n=4 per group, * *p*<0.05 vs CTR, # *p*<0.05 vs noDR.

Fig. 4 Ang 1 and HIF-1α mRNA and protein expressions in plasma EVs extracted from healthy subjects (**CTR**) and from diabetic patients without (**noDR**) and with retinopathy (**DR**), fold increases vs the control group (CTR). *White bars*: CTR, *light grey bars*: noDR, *dark grey bars*: DR. **a**) **Ang-1** and **b**) **HIF-1α mRNA expression**, n=7 per group, * p<0.05 vs CTR; **c-e**) **Ang-1** and **d-f**) **HIF-1α protein expression**: **c-d**) quantitative analysis, n=7 per group, * *p*<0.05 vs CTR, # *p*<0.05 vs noDR; **e-f**) representative images of one relevant Western blot.

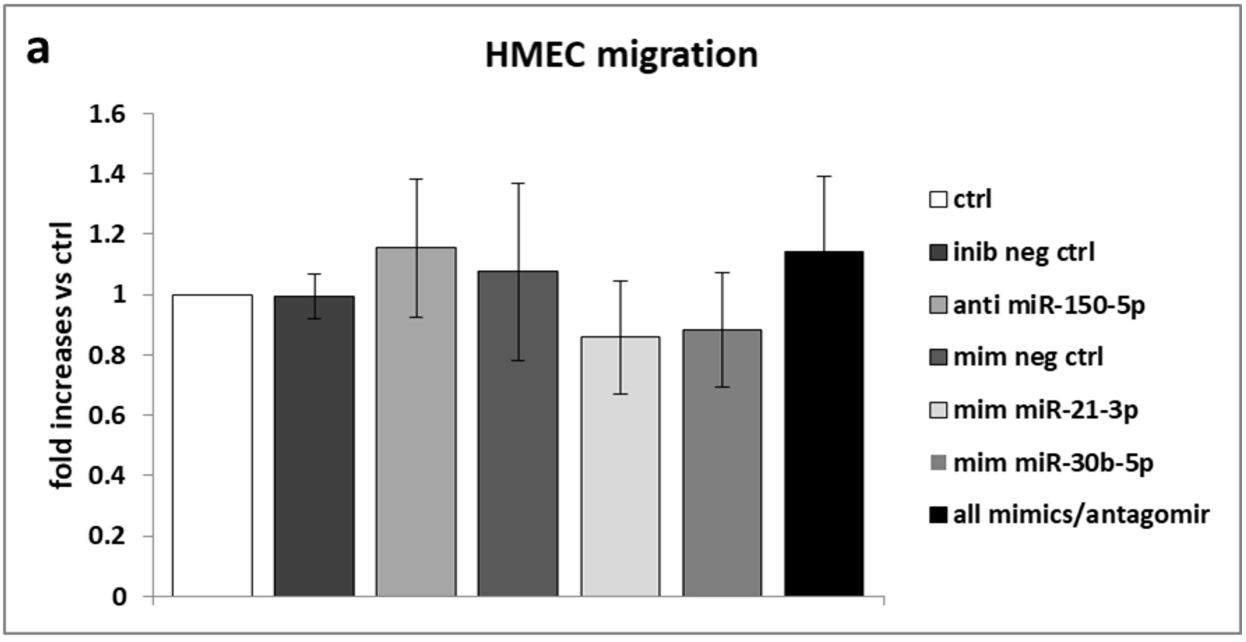
a
HMEC migration
fold increases vs ctrl
1.6
1.4
1.2
1
0.8
0.6
0.4
0.2
0
ctrl
inib neg ctrl
anti miR-150-5p
mim neg ctrl
mim miR-21-3p
mim miR-30b-5p
all mimics/antagomir

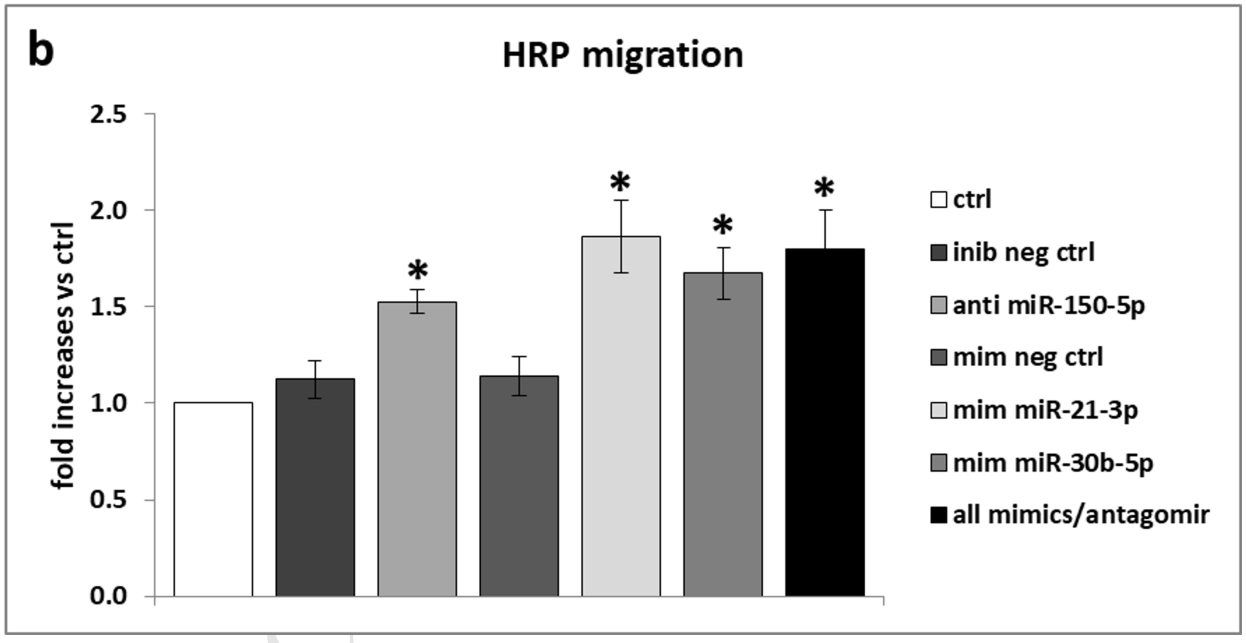
b
HRP migration
fold increases vs ctrl
2.5
2.0
1.5
1.0
0.5
0.0
*
*
*
ctrl
inib neg ctrl
anti miR-150-5p
mim neg ctrl
mim miR-21-3p
mim miR-30b-5p
all mimics/antagomir

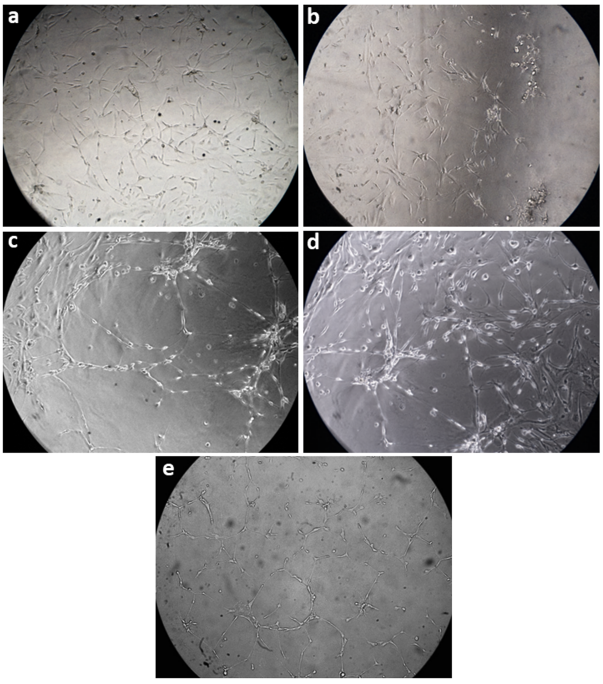

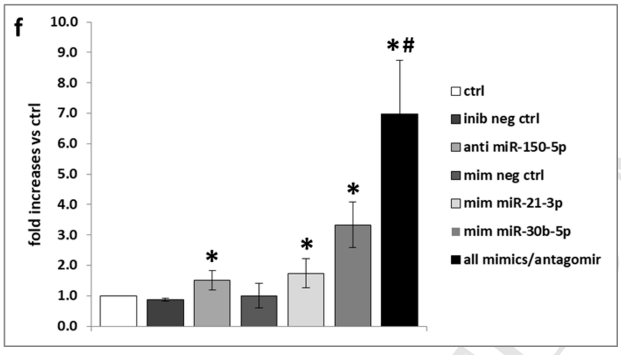

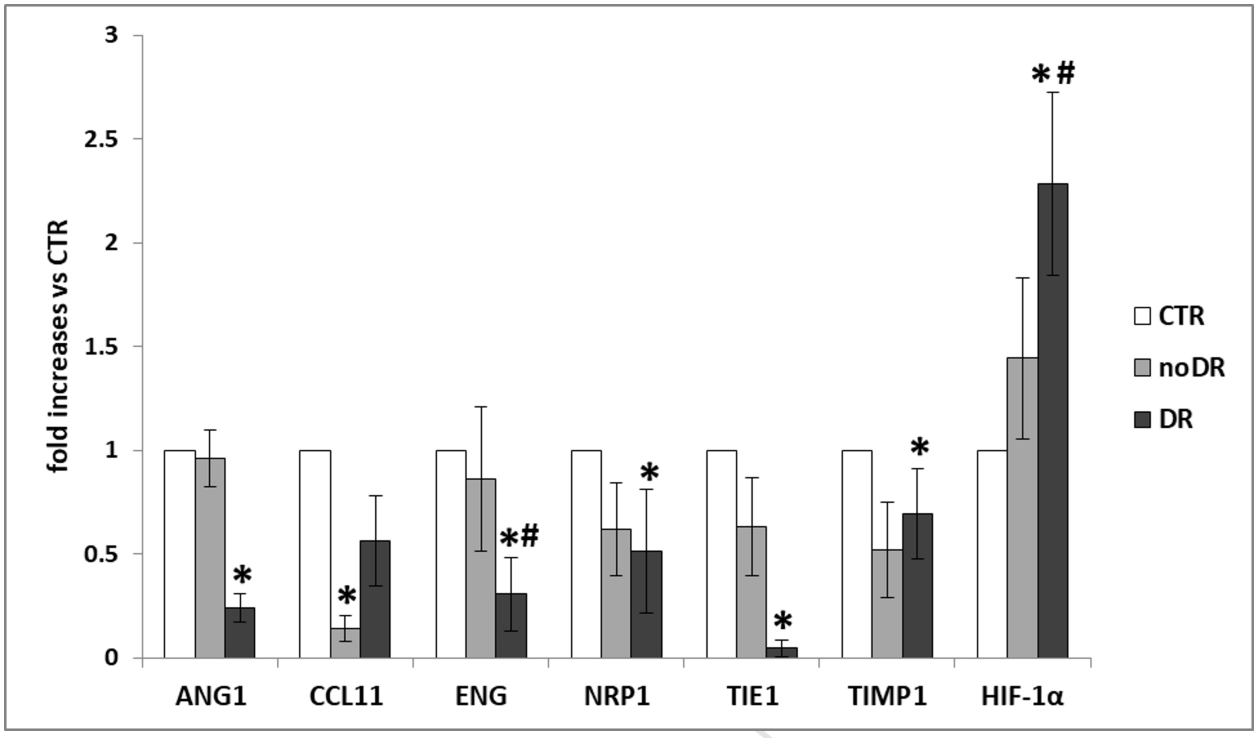

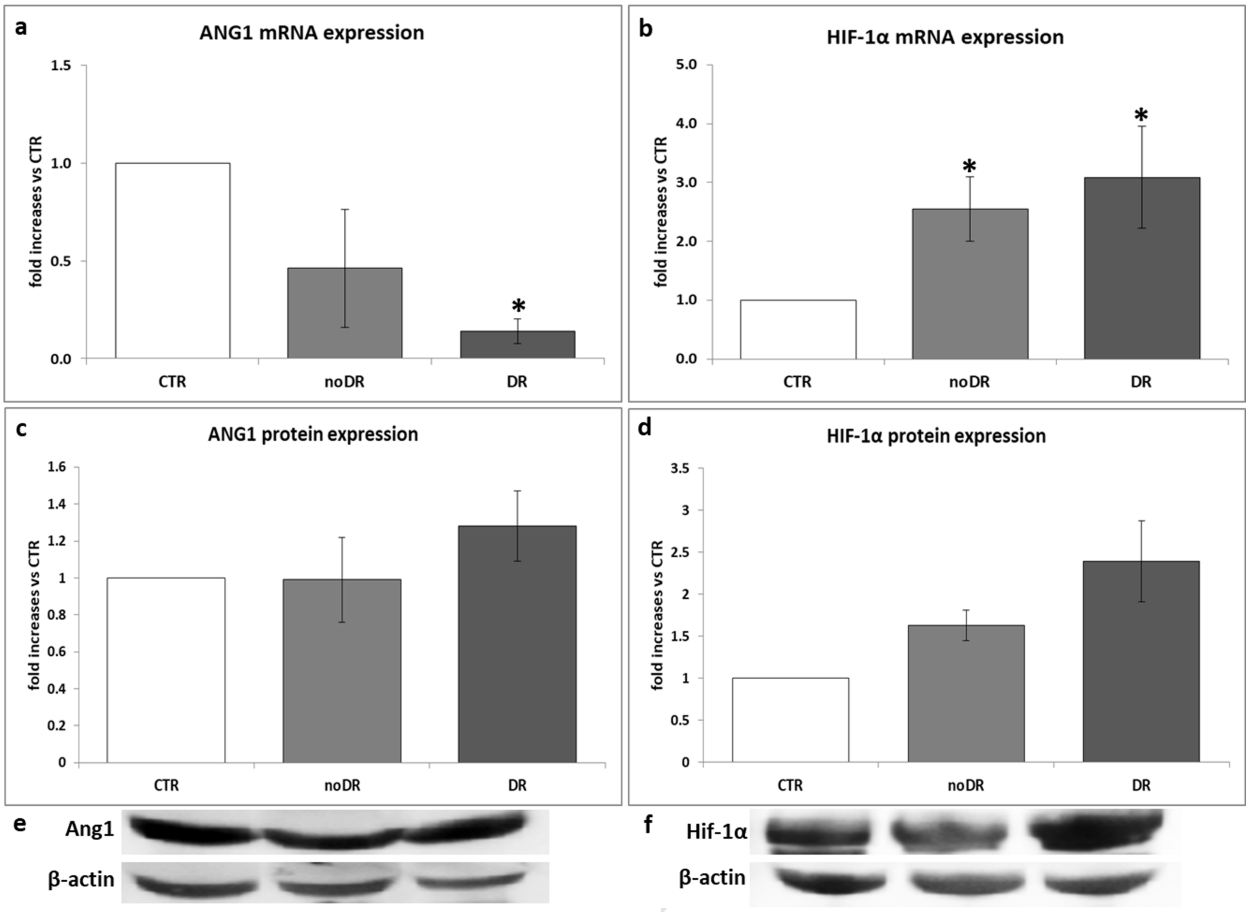

Mazzeo et al.: ***Functional analysis of miR-21-3p, miR-30b-5p and miR-150-5p shuttled by extracellular vesicles from diabetic subjects reveals their association with diabetic retinopathy***

Highlights

- Prognostic biomarkers for diabetic retinopathy are needed
- Functional studies confirm miR-150-5p, miR-21-3p, miR-30b-5p involvement
- HIF-1α is also increased in extracellular vesicles from diabetic retinopathy subjects
- miR-150-5p, miR-21-3p, miR-30b-5p and HIF-1α concur to hypoxia-induced angiogenesis
- Intra-vesicle miR-150-5p, miR-21-3p, miR-30b-5p as biomarkers of diabetic retinopathy